development during the Holocene. For instance, climatic shifts since the late Pleistocene may have played a part in causing high rates of mammal extinctions reported for the West Indies[28]. Furthermore, abrupt climate fluctuations during the late Holocene may have influenced the development of prehistoric cultures in the Caribbean and nearby Mesoamerica. Testing the regional significance of the climate changes outlined here will require similar high-resolution studies in other lowland Neotropical lakes. □

Received 15 April; accepted 9 July 1991.

1. Brenner, M. & Binford, M. W. *J. Paleolimnol.* **1,** 85-97 (1988).
2. Gasse, F., Téhet, R., Durand, A., Gibert, E. & Fontes, J. C. *Nature* **346,** 141-146 (1990).
3. Fontes, J. C. & Gonfiantini, R. *Earth planet. Sci. Lett.* **3,** 258-266 (1967).
4. Higuera-Gundy, A. thesis, Univ. of Florida (1991).
5. Broecker, W. S. *et al. Paleoceanography* **3,** 1-19 (1988).
6. Street-Perrott, F. A. & Perrott, R. A. *Nature* **343,** 607-612 (1990).
7. Bradbury, J. P. *et al. Science* **214,** 1299-1305 (1981).
8. Deevey, E. S., Brenner, M. & Binford, M. W. *Hydrobiologia* **103,** 211-216 (1983).
9. Gasse, F., LeDee, V., Massault, M. & Fontes, J. *Nature* **342,** 57-65 (1989).
10. Leyden, B. W. *Proc. natn. Acad. Sci.* **81,** 4856-4859 (1984).
11. Leyden, B. W. *Ecology* **66,** 1279-1295 (1985).
12. Piperno, D. R., Bush, M. B & Colinvaux, P. A. *Quat. Res.* **33,** 108-116 (1990).
13. Street, F. A. & Grove, A. T. *Nature* **261,** 385-390 (1976).
14. Street, F. A. & Grove, A. T. *Quat. Res.* **12,** 83-118 (1979).
15. Watts, W. A. *Geology* **3,** 344-346 (1975).
16. Duplessy, J.-C. Delibrias, G., Turon, J. L., Pujol, C. & Duprat, J. *Palaeogeogr. Palaeoclim. Palaeoecol.* **35,** 121-144 (1981).
17. Duplessy, J.-C. *et al. Nature* **320,** 350-352 (1986).
18. Jansen, E. & Veum, T. *Nature* **343,** 612-616 (1990).
19. Leyden, B. W. *Quat. Res.* **81,** 407-414 (1987).
20. Street-Perrott, F. A. & Harrison, S. P. in *Paleoclimate Analysis and Modeling* (ed. Hecht, A. D.) 291-340 (Wiley, New York, 1985).
21. Kutzbach, J. E. & Street-Perrott, F. A. *Nature* **317,** 130-134 (1985).
22. Hastenrath, S. *J. atm. Sci.* **33,** 202-215 (1976).
23. Hastenrath, S. *Mon. Weath. Rev.* **112,** 1097-1107 (1984).
24. Manabe, S. & Hahn, D. G. *J. geophys. Res.* **82,** 3889-3911 (1977).
25. Gates, W. L. *Science* **191,** 1138-1144 (1976).
26. Kutzbach, J. E. *Science* **214,** 59-61 (1981).
27. Kutzbach, J. E. & Guetter, P. J. in *Milankovitch and Climate, Understanding the Response to Astronomical Forcing, Part 2* (eds Berger, A. L., Imbrie, J., Hays, J., Kukla, G. & Saltzman, B.) 801-820 (Reidel, Dordrecht/Hingham, 1984).
28. Morgan, G. S. & Woods, C. A. *Biol. J. Linnaean Soc.* **28,** 167-203 (1986).
29. Gagnon, A. R. & Jones, G. A. *Radiocarbon* **33,** 198 (1991).
30. Deevey, E. S. & Stuiver, M. *Limnol. Oceanogr.* **9,** 1-11 (1964).
31. Berger, A. *Inst. d'Astr. Géophys. G. Lemaitre Contrib.* 37 (Univ. Catholique, Louvain-la-Neuve, Belgium, 1978).
32. Klein, J., Lermann, J. C., Damon, P. E. & Ralph, E. K. *Radiocarbon* **24,** 103-150 (1982).
33. Bard, E., Hamelin, B., Fairbanks, R. G. & Zindler, A. *Nature* **345,** 405-410 (1990).

ACKNOWLEDGEMENTS. We thank R. Forester for ostracod identification. This work is dedicated to the late E. Deevey. This research was supported by the NSF (D.A.H., M.W.B. and E. S. Deevey), NASA (J.H.C.) and a Whitehall Foundation grant awarded to E.S. Deevey. Accelerator radiocarbon analyses were done at the NSF Accelerator Facility at the University of Arizona.

Dispersion and advection in unsaturated porous media enhanced by anion exclusion

H. Gvirtzman* & S. M. Gorelick

Department of Applied Earth Sciences, Stanford University, Stanford, California 94305, USA

IT has been observed[1-4] that the average transport velocity of dissolved anions through soils may be larger than that of the accompanying water molecules, owing to electrostatic repulsion by negatively charged solid surfaces, which forces the anions into pore centres where the velocity is faster. This phenomenon, known as anion exclusion, has been explained by diffusive double-layer theory[5-7]. Here we present analyses and numerical modelling of concentration/depth profiles of tritium, chloride and sulphate which were collected from irrigated land in the Israeli coastal plain. We found that the anions travelled at about twice the velocity of tritium. The behaviour of tritium is consistent with advective–diffusive transport, but the values of the dispersion coefficients associated with anion transport greatly exceeded the values expected for molecular diffusion in a porous medium, and were ~30 times those found for tritium transport. Our results indicate that anion exclusion restricts the number of active pore networks available for anion transport. We present two conceptual models that can explain the observed results—in one model some porous regions are completely blocked, whereas in the other they are only partially blocked.

The phenomenon of anion exclusion has been demonstrated in experimental studies[1-4] and has been explained by diffusive double-layer theory[5-7]. As a result of anion exclusion, the average transport velocity of dissolved anions through soils may be larger than that of the accompanying water molecules because of electrostatic repulsion by negatively charged solid surfaces which forces the anions into the pore centres where the velocity is faster. As recognized here, exclusion may greatly reduce the amplitude between extreme values in the anion concentration profiles, which can be described by enhanced dispersion.

During a field investigation of an irrigated region, 10 km north of Tel-Aviv[8], solute migration was studied. Precipitation and irrigation each had characteristic chemical source-signatures. The 27-yr chronological record of source events is imprinted in the depth profile of solute concentration in the sediment. Concentration peaks and minima corresponding to winter rains and summer irrigation were identified and dated. The vertical profile consists of 27.5 m of water-unsaturated sediments. Three horizons characterize the profile: (1) the upper 0.9-m soil unit, (2) a 9-m-thick clay loam layer and (3) an underlying homogeneous sandy layer that extends down to the water table. The boundary between each zone is characterized by an abrupt change in the unsaturated water content. The influence of the capillary fringe extended ~2.5 m above the water table.

Figure 1 shows solute data consisting of concentrations of tritium, chloride and sulphate that were measured in the extracted solution of samples collected along the profile. Atmospheric thermonuclear tests during the 1950s and 1960s caused rainwater to become enriched in tritium. This rainwater then infiltrated the soil. The history of the tritium concentrations in rain is known in this region[8] as it is in many locations throughout the world[9]. Isotopic enrichment of tritium due to transpiration is negligible[10]. The source of chloride was irrigation water derived from sewage effluent high in chloride. Sulphate was a component of ammonium sulphate fertilizer. The average recharge of 150 mm yr^{-1} is 17% of the total rate of applied water. The rest is evapotranspired. Seasonal wetting and drying affects the upper soil, but can be neglected below 2 m where steady-flow conditions exist.

The peaks in the three concentration profiles were correlated with their seasonal chronological input events. From the vertical separation of the peaks and initial simulations, we determined the average vertical velocities through the lithologic zones (Table 1).

The three sets of concentration data were successfully reproduced using two different conceptual models. First is the 'dispersion model' which involves transient one-dimensional advective–dispersive transport under steady-flow conditions. For tritium, first-order kinetic decay was included. To represent the effects of anion exclusion, anion transport was divided into two regimes: an excluded volume near the solid surfaces containing no anions, and a mobile volume in which all of the anions are concentrated. The general governing equation[3] is

$$(\theta-\theta_{ex})\frac{\partial C}{\partial t}=\frac{\partial}{\partial z}\left[(\theta-\theta_{ex})D_h\frac{\partial C}{\partial z}\right]-Q\frac{\partial C}{\partial z}-(\theta-\theta_{ex})\lambda C \qquad (1)$$

where θ is the unsaturated water content (dimensions L^3/L^3); θ_{ex} is the water content of the excluded volume (L^3/L^3) (θ_{ex} is zero for tritium, and the water content of the mobile domain is $\theta_m=\theta-\theta_{ex}$); C is the solute concentration (M/L^3); D_h is the hydrodynamic dispersion coefficient, $D_h(z)$ (L^2/T); Q is the

* Present address: Institute of Earth Sciences, Hebrew University, Givat Ram, Jerusalem 91904, Israel.

TABLE 1 Transport parameter values for clay-loam zone

	Dispersion model					Exchange model					
Solute	E_i	θ_m	θ_{ex}	V (cm d^{-1})	D_h (cm^2 d^{-1})	D_d (cm^2 d^{-1})	D_p (cm^2 d^{-1})	V' (cm d^{-1})	θ_{ex}	θ_{im}	α (1/d)
^3H	1.00	0.190†	0.000	0.202‡	0.072±0.01§	1.469‖	0.072#	0.202	0.000††	0.000	—
Cl^-	0.56*	0.106	0.084	0.360‡	1.67±0.25§	1.296¶	0.036**	0.439††	0.061‡‡	0.023±0.004§	0.0034±0.0012§
SO_4^{2-}	0.46*	0.087	0.103	0.440‡	2.93±0.95§	0.657¶	0.015**	0.537††	0.084‡‡	0.019±0.005§	0.0024±0.0013§

* Mobile fraction = velocity of tritium/velocity of anion.
† For tritium, the total water content is mobile.
‡ Based on peak separation, Fig. 1.
§ Calibrated value and standard deviation of estimate.
‖ Taken at 13 °C (ref. 21).
¶ Taken at 13 °C (ref. 22).
# Calibrated value D_h from dispersion model.
** Microscale tortuosity, 0.05, calculated using equation (2) for tritium and applied to anions as dispersion coefficient in exchange model.
†† Actual anion average velocity, V', is the product of the apparent velocity, V, based on peak separation and $(1+\theta_{im}/\theta_m)$.
‡‡ $\theta_{ex}=\theta-\theta_m-\theta_{im}$.

darcian flux (L/T) related to the average velocity, V, by $V=Q/(\theta-\theta_{ex})$; λ is the first-order kinetic decay rate for tritium (1/T); t is time (T); and z is vertical distance (L) along the flow direction.

For average velocities of tritium seen here, mechanical dispersion is negligible with respect to molecular diffusion[11,12]. The molecular diffusion coefficient in porous media, $D_p(L^2/T)$, is related to the diffusion coefficient in a free fluid, $D_d(L^2/T)$, by

$$D_p = D_d \tau E_i \quad (2)$$

where τ (where $\tau<1.0$) is tortuosity[13], and E_i is the fraction of the unsaturated water content associated with transport of anion i ($E_i=1.0$ for tritium). The mobile fraction, $E_i=\theta_m/\theta=V_{tritium}/V_{anion}$, is obtained from the relationship, $V_{anion}\theta_m=V_{tritium}\theta$.

Second is the 'exchange model', which involves advective-diffusive transport of anions in the mobile domain plus diffusional exchange with an immobile domain. The water content of the immobile domain is θ_{im}, and the excluded portion is θ_{ex}. The total unsaturated water content is now defined as

$$\theta = \theta_{ex} + \theta_m + \theta_{im} \quad (3)$$

The coupled governing equations for the mobile and immobile domains are

$$\theta_m \frac{\partial C_m}{\partial t} = \frac{\partial}{\partial z}\left[\theta_m D_p \frac{\partial C_m}{\partial z}\right] - Q\frac{\partial C_m}{\partial z} - \theta_m \alpha (C_m - C_{im}) \quad (4)$$

$$\theta_{im} \frac{\partial C_{im}}{\partial t} = \theta_m \alpha (C_m - C_{im}) \quad (5)$$

where C_m and C_{im} are the anion concentrations in the mobile and immobile domains; and α is the mass transfer rate coefficient between the mobile and immobile domains (1/T).

The governing equations were solved numerically using the finite element method with 48,000 spatial nodes and 200 time steps per year. Inflow was modelled using a series of 54 seasonal solute flux values, corresponding to alternating winters and summers during the years 1957–84. The duration of each season was adjusted during calibration but was tightly limited because any single change in the duration of a winter or summer affected all three independently simulated profiles. Values below 25 m, influenced by the capillary fringe, were disregarded. Calibration employed simulation combined with nonlinear extreme-value weighted least-squares regression[14].

Figure 1*a–c* shows the calibrated simulations using the 'dispersion model' and the field data for tritium, chloride, and sulphate concentrations along the profile after 27 yr of transport (1957–84). The values of the dispersion coefficients were calibrated in the clay-loam and fixed in the sand at their values of molecular diffusion in porous media (Table 1). In the sand, tritium and anions had the same velocity. In the clay-loam, however, the average velocity of the three constituents increased in the order tritium to chloride to sulphate. The greater the charge, the greater the repulsive forces from the charged surfaces. The D_h value for tritium in both sediment horizons and the values of D_h for the anions in the sand are consistent with values of molecular diffusion in porous media (Table 1). The D_h values for the anions in the clay-loam layer, however, were 23 and 41 times that of tritium. Sensitivity analyses, using the D_h value of tritium to simulate anion transport, doubled the range of concentration values along the profile compared with the anion field data.

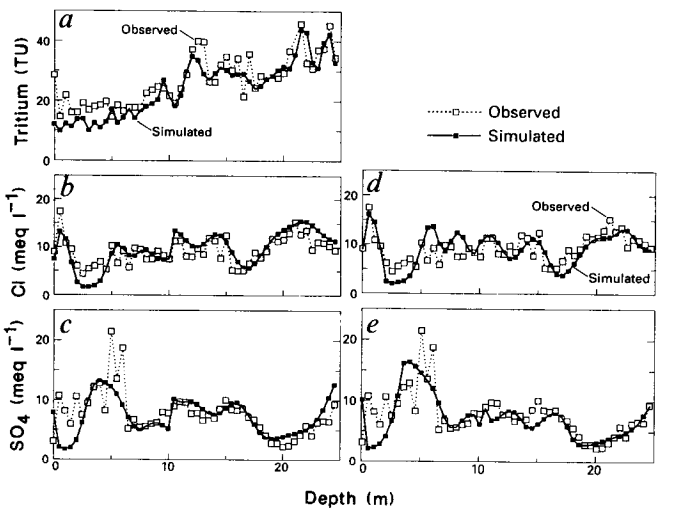

FIG. 1 Comparisons of simulated concentrations with field data for *a*, tritium, *b*, chloride and *c*, sulphate using the 'dispersion model', and for *d*, chloride and *e*, sulphate using the 'exchange model'. Simulations *a–c* were based on a finite-element solution to the governing advective-dispersive equation, whereas *d* and *e* were based on the finite-element solution to the coupled mobile-immobile domain transport equations. Parameter values associated with the clay-loam layer for the two simulation models are shown in Table 1. In the sand/sandstone unit the solute velocity for all three constituents was 0.50 cm d^{-1}, and the hydrodynamic dispersion coefficient was 0.05 cm^2 d^{-1}.

METHODS. Tritium was measured by low-level β-counting and values are given in tritium units (TU) where 1 TU corresponds to 1 atom per 10^{18} hydrogen atoms. Chloride and sulphate were measured by ion chromatography using high-pressure liquid chromatography[8]. Gravimetric water content was measured by weighing the sample before and after drying. Volumetric water content was calculated using bulk density values of 1.55 and 1.28 g cm^{-3} for clay loam and sand, respectively.

Figure 1*d*, *e* shows the calibrated simulation results using the 'exchange model' (Table 1). This model was used only to simulate anion transport. Tritium transport was described using the 'dispersion model'. The dispersion coefficients were fixed at their values of molecular diffusion, D_p (Table 1). Diffusional exchange reduces the advective velocity because the anions spend some time in the immobile domain. Anion velocity was related to the fractional water content of the immobile versus mobile domains (Table 1). Calibrated parameters for the 'exchange model' are θ_{im} and α. Compared with the monovalent ion, exclusion of the divalent ion may generate smaller immobile pockets (smaller θ_{im}) with narrower passages through which diffusive exchange with the mobile domain occurs (smaller rate coefficient, α).

The value of the apparent dispersion coefficient used in the 'dispersion model' was calculated to within 10% of the parameter estimate when using[15]

$$D_h = \frac{\theta_m}{\theta_m + \theta_{im}}\left[D_p + \frac{V^2}{\alpha}\left(\frac{\theta_{im}}{\theta_m + \theta_{im}}\right)^2\right] \quad (6)$$

with the values of parameters in the 'exchange model'.

The effect we document shows that, compared with tritium transport, anion advection is doubled, and attenuation of the anion concentration profiles is greatly enhanced. Both effects are believed to be caused by anion exclusion.

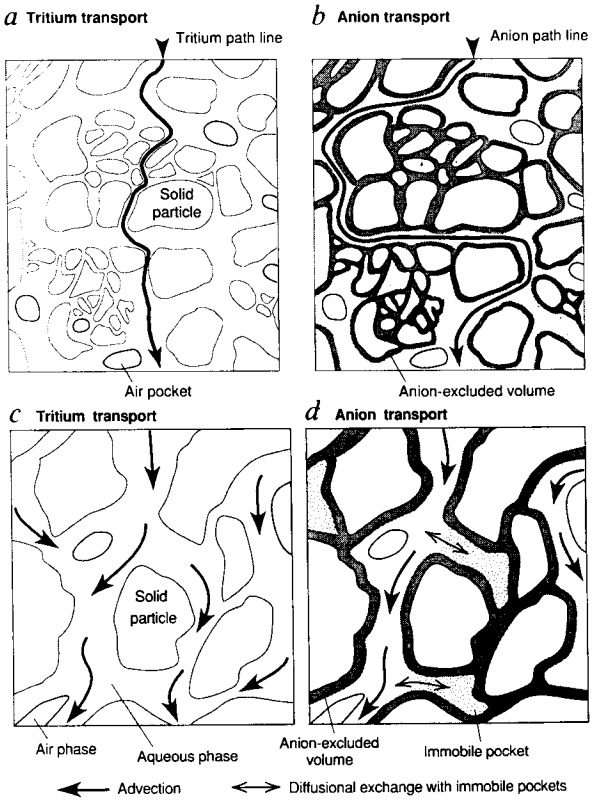

FIG. 2 Schematic model of pore-scale flow networks controlling migration according to the 'dispersion model', *a*, *b*, and the 'exchange model', *c*, *d*. Electrostatic forces repel anions from negatively charged surfaces, thereby excluding them from the small pores of the unsaturated porous medium. In the 'dispersion model' anions necessarily follow a more tortuous pathway compared with that of tritium, which is not subject to ion exclusion. Dispersion coefficient values associated with the transport of anions are much greater than that of tritium, perhaps, because anions 'see' an effectively more heterogeneous porous medium. In the 'exchange model' anion exclusion creates isolated dead-end pockets which are connected to the mobile domain by larger pore passageways through which diffusional exchange occurs. Tritium is not excluded from the small pores and flows freely through the entire network.

The 'dispersion model' generates attenuation by permitting increased mechanical dispersion. Values of dispersion coefficients for chloride and sulphate exceed their values of molecular diffusion coefficients in the porous medium by 46 and 195 times, respectively. Yet tritium transport behaviour was successfully reproduced by a model of molecular diffusion alone. It is evident that anion transport must involve some means of attenuating extreme values of concentration that cannot solely be caused by molecular diffusion.

Perhaps anion exclusion creates enhanced dispersion by generating heterogeneities that serve as flow barriers. Figure 2*a*, *b* shows a single porous medium and compares the active flow network for tritium with that for anions. Tritium is able to flow through both large and small pores. On the other hand, anions are excluded from small pores, which may be concentrated in aggregates. Anion flow, which is restricted to the larger pores, will be more tortuous than that of tritium because of the aggregated obstacles. The larger dispersion coefficients for anions may reflect this additional velocity variation due to heterogeneity[16–18].

An alternative explanation employs the 'exchange model' which generates attenuation by allowing for immobile zones that are created during anion transport. Figure 2*c*, *d* compares the flow network for tritium with that for anions. Tritium flow is unrestricted, whereas anions are excluded from small pores, thereby creating nearly isolated immobile pockets that are connected to the mobile zone by larger pores. Mass transfer between the mobile and immobile zones attenuates extreme values of concentration. Using this model, an immobile fraction occupying about one-tenth of the total water content best reproduced the concentration data. The values of the mass transfer coefficient were found to be two to three orders of magnitude less than those reported from laboratory studies[15,19,20]. Model results indicate that compared with the monovalent ion (chloride), the divalent anion (sulphate), has a greater exclusion volume surrounding the clay surfaces, smaller dead-end pockets, and smaller passageways through which mass transfer occurs.

Of most significance is the fundamental similarity between the two conceptual models. Both models maintain that anion exclusion greatly influences the active porous network. Because anions cannot flow through small pores, some porous regions may be completely blocked ('dispersion model') or partially blocked ('exchange model'). The geometry of blockages is the significant difference between the two models. For both conceptual models there are restricted active flow networks experienced by anions during transport which enhance the attenuation of extreme values in the concentration profiles. □

Received 15 February; accepted 12 July 1991.

1. Mokady, R. S., Ravina, J. & Zazlavsky, D. *Israel J. Chem.* **6**, 159–165 (1968).
2. Smith, S. J. *Soil Sci.* **114**, 259–263 (1972).
3. James, R. V. & Rubin, J. *Soil Sci. Soc. Am. J.* **50**, 1142–1149 (1986).
4. Bond, W. J. & Phillips, J. R. *Soil Sci. Soc. Am. J.* **54**, 633–645 (1990).
5. De Haan, F. A. M. *Centrum voor Landbouwpublikaties en Landbouwdocumentatie*, 164 (Wageningen, 1965).
6. Krupp, H. K., Biggar, J. W. & Nielsen, D. R. *Soil Sci. Soc. Am. Proc.* **36**, 412–417 (1972).
7. Bresler, E. *Soil Sci. Soc. Am. Proc.* **37**, 663–669 (1973).
8. Gvirtzman, H., Ronen, D. & Magaritz, M. *J. Hydrol.* **87**, 267–283 (1986).
9. Gat, R. J. *Handbook of Environmental Isotope Geochemistry* vol. **1**, 21–47 (Elsevier, Amsterdam, 1980).
10. Zimmermann, U. *Science*, **152**, 346–347 (1966).
11. Bear, J. *Dynamics of Fluids in Porous Media*, 764p (Elsevier, New York, 1972).
12. Pfankuch, H. D. *Rev. Inst. Fr. Petrol.* **2**, 215–270 (1963).
13. Marsily, G. de, *Quantitative Hydrogeology*, 440p (Academic Press, Orlando, 1986).
14. Wagner, B. J. & Gorelick, S. M. *Water Resource Res.* **22**, 1303–1315 (1986).
15. DeSmedt, F., Wauters, F. & Sevilla, S. *J. Hydrol.* **85**, 169–181 (1986).
16. Dagan, G. *Water Resource Res.* **22**, 120S–134S (1986).
17. Gelhar, L. W. *Water Resource Res.* **22**, 135S–145S (1986).
18. Neuman, S. P. *Water Resource Res.* **26**, 1749–1758 (1990).
19. Van Genuchten, M. T. & Wierenga, P. J. *Soil Sci. Soc. Am. J.* **41**, 272–285 (1977).
20. Rao, P. S. C., Jessup, R. E., Rolston, D. E., Davidson, J. M. & Kilcrease, D. P. *Soil Sci. Soc. Am. J.* **44**, 684–688 (1980).
21. Wang, J. H., Robinson, C. V. & Edelman, I. S. *J. Am. chem. Soc.* **75**, 466–470 (1953).
22. Li, Y. H. & Gregory, S. *Geochim. cosmochim. Acta* **38**, 703–714 (1974).

ACKNOWLEDGEMENTS. We thank G. de Marsily, G. Garvin, G. Hornberger, and L. Konikow for their review comments. We thank the Dr. Chaim Weizmann Fellowship Program, Israel, the NSF for their support of this research and the Hewlett-Packard Company for their grant of computer equipment.